Accepted Manuscript

Title: Synthesis of new heterometallic complexes by tin-sulfur bond cleavage of $pySSnPh_3$ (pySH = pyridine-2-thiol) at triruthenium and triosmium centres

Authors: Arun K. Raha, Shishir Ghosh, Iqbal Hossain, Shariff E. Kabir, Brian K. Nicholson, Graeme Hogarth, Luca Salassa

PII: S0022-328X(10)00729-1

DOI: 10.1016/j.jorganchem.2010.11.022

Reference: JOM 16882

To appear in: *Journal of Organometallic Chemistry*

Received Date: 9 October 2010

Revised Date: 13 November 2010

Accepted Date: 15 November 2010

Please cite this article as: A.K. Raha, S. Ghosh, I. Hossain, S.E. Kabir, B.K. Nicholson, G. Hogarth, L. Salassa. Synthesis of new heterometallic complexes by tin-sulfur bond cleavage of $pySSnPh_3$ (pySH = pyridine-2-thiol) at triruthenium and triosmium centres, Journal of Organometallic Chemistry (2010), doi: 10.1016/j.jorganchem.2010.11.022

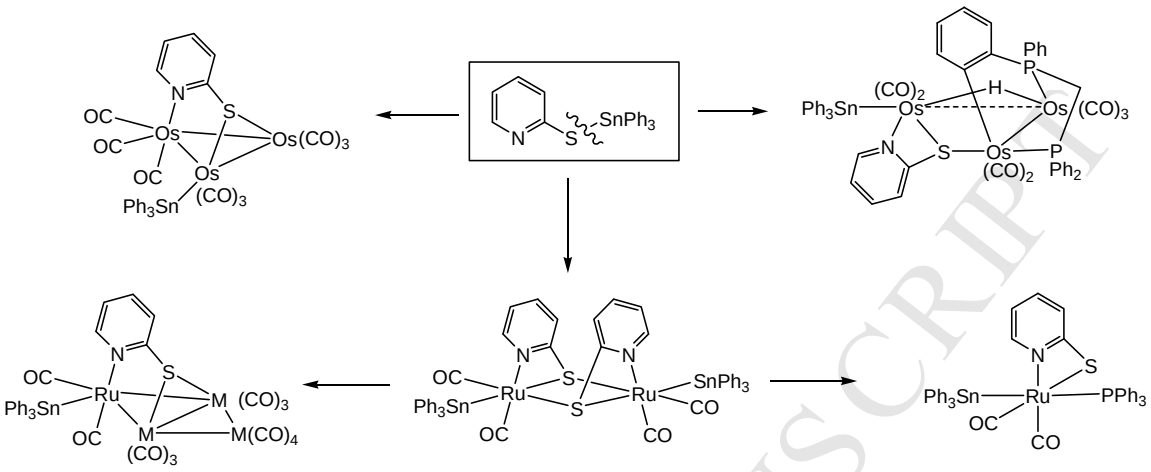

The reactivity of $pySSnPh_3$ with triruthenium and triosmium carbonyl clusters has been investigated. A number of novel clusters enriched with tin and sulfur donor ligands have been obtained.

Synthesis of new heterometallic complexes by tin-sulfur bond cleavage of $pySSnPh_3$ (pySH = pyridine-2-thiol) at triruthenium and triosmium centres

Arun K. Raha [a], Shishir Ghosh [a], Iqbal Hossain [a], Shariff E. Kabir [a,*], Brian K. Nicholson [b], Graeme Hogarth [c], Luca Salassa [d]

[a] *Department of Chemistry, Jahangirnagar University, Savar, Dhaka-1342, Bangladesh*

[b] *Department of Chemistry, University of Waikato, Hamilton, New Zealand*

[c] *Department of Chemistry, University College London, 20 Gordon Street, London WC1H OAJ, UK*

[d] *Department of Chemistry, University of Warwick, Gibbet Hill Road, Coventry CV4 7AL, UK*

Abstract

The ruthenium-tin complex, $[Ru_2(CO)_4(SnPh_3)_2(\mu\text{-}pyS)_2]$ (**1**), the main product of the oxidative-addition of $pySSnPh_3$ to $Ru_3(CO)_{12}$ in refluxing benzene, is $[Ru(CO)_2(pyS)(SnPh_3)]$ synthon. It reacts with PPh_3 to give $[Ru(CO)_2(SnPh_3)(PPh_3)(\mu\text{-}pyS)]$ (**2**) and further with $Ru_3(CO)_{12}$ or $[Os_3(CO)_{10}(NCMe)_2]$ to afford the butterfly clusters $[MOs_3(CO)_{12}(SnPh_3)(\mu_3\text{-}pyS)]$ (**3-4**). Direct addition of $pySSnPh_3$ to $[Os_3(CO)_{10}(NCMe)_2]$ at 70^oC gives $[Os_3(CO)_9(SnPh_3)(\mu_3\text{-}pyS)]$ (**5**) as the only bimetallic compound, while with unsaturated $[Os_3(CO)_8\{\mu_3\text{-}PPh_2CH_2P(Ph)C_6H_4\}(\mu\text{-}H)]$ the previously reported $[Os_3(CO)_8(\mu\text{-}pyS)(\mu\text{-}H)(\mu\text{-}dppm)]$ (**6**) and the new bimetallic cluster $[Os_3(CO)_7(SnPh_3)\{\mu\text{-}Ph_2PCH_2P(Ph)C_6H_4\}(\mu\text{-}pyS)[(\mu\text{-}H)]$ (**7**) are formed at 110^oC. Compounds **1**, **2**, **4**, **5** and **7** have been characterized by X-ray diffraction studies.

Keywords: $pySSnPh_3$; Tin-sulfur bond cleavage; Butterfly clusters, Mixed-metal cluster; X-ray structure.

1. Introduction

Transition metal-tin complexes have attracted considerable interest primarily because tin can be used to modify bimetallic catalysts, improving their reactivity and product selectivity in a variety of chemical transformations [1-13]. Further it has recently been found that the binding of metallic nanoparticles to oxide supports can be enhanced by the incorporation of tin [10-14]. There are several methods for the incorporation of tin into transition metal complexes. The most widely used method is the oxidative-addition of organotin hydrides and using this methodology a number of transition metal-tin clusters with intriguing structural features have been synthesized, as exemplified by the work of Adams and co-workers [15-26]. More recently other tin-element oxidative-addition reactions have been exploited, for example Gárate-Morales and Fernández-G have prepared amine-containing osmium-tin compounds *via* the cleavage of the nitrogen-tin bond in aminostannanes [27-29]. Our group have shown that tetraphenylthiostannane is an excellent source for the inclusion of both tin and sulfur atoms into transition metal clusters [30], reaction of $Ru_3(CO)_{12}$ with Ph_3Sn-SPh affording bimetallic $[Ru_3(CO)_8(SnPh_3)_2(\mu_3\text{-}SnPh_2)(\mu\text{-}SPh)_2]$ resulting from both tin-sulfur and tin-carbon bond cleavage (Scheme 1) [30, 31].

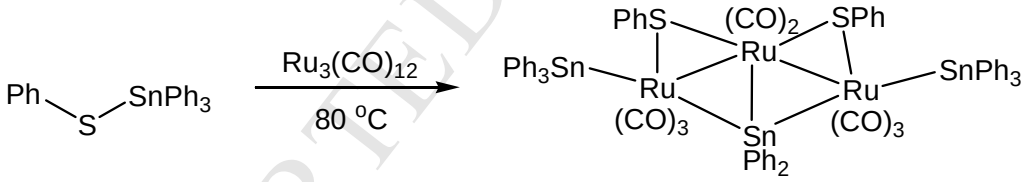

Scheme 1.

If tin-containing transition metal clusters are to be used towards the synthesis of catalytically-active nanoparticles then facile and high-yielding routes to these clusters is a necessity [32]. We were encouraged by the facile nature of the tin-sulfur bond cleavage (Scheme 1) but sought to limit this to a single addition rather than the multiple addition products found with Ph_3Sn-SPh. In order to do this we considered the introduction of a thiolate-ligand with secondary binding sites and consequently we have investigated reactions of pyridine-2-thiolate-triphenyltin (pyS-$SnPh_3$) with triruthenium and triosmium clusters. Thus, in contrast to the phenylsulfide ligand which generally acts either as a terminal one-electron, or bridging three-electron, donor ligand, the pyridine-2-thiolate ligand (pyS) can coordinate to metal centers in a wide variety of ways (Chart 1) which in turn is expected to influence the nature of the products

formed. Indeed this is the case as we have found that the presence of the coordinating nitrogen atom substantially affects the course of the reactions and we obtained a completely different set of products to the related reactions with PhS-$SnPh_3$. These findings are presented herein.

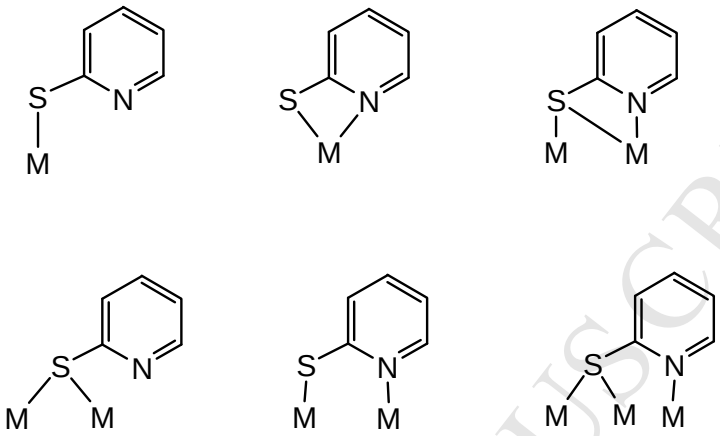

Chart 1.

2. Experimental section

All the reactions were carried out under a nitrogen atmosphere using standard Schlenk techniques. Reagent-grade solvents were dried using appropriate drying agents and were freshly distilled prior to use by standard methods. $Os_3(CO)_{12}$ and $Ru_3(CO)_{12}$ were purchased from Strem Chemicals Inc. and used without further purification, $[Os_3(CO)_{10}(NCMe)_2]$ [33], $[Os_3(CO)_8\{\mu_3\text{-}PPh_2CH_2P(Ph)C_6H_4\}(\mu\text{-}H)]$ [34] and $pySSnPh_3$ [31, 35, 36] were prepared according to the literature procedures. Pyridine-2-thiol, Ph_3SnCl and PPh_3 were purchased from Aldrich and used as received. Infrared spectra were recorded on a Shimadzu FTIR 8101 spectrophotometer. ^1H NMR spectra were recorded on a Bruker DPX 400 instrument. All chemical shifts are reported in δ units with reference to the residual protons of the deuterated solvents. Fast atom bombardment mass spectra were obtained on a JEOLSX-102 spectrometer using 3-nitrobenzyl alcohol as matrix and CsI as calibrant.

2.1. Reaction of $Ru_3(CO)_{12}$ with $pySSnPh_3$ - To a benzene solution (30 mL) of $Ru_3(CO)_{12}$ (100 mg, 0.156 mmol) was added $pySSnPh_3$ (147 mg, 0.319 mmol) and the reaction mixture was heated to reflux for 45 min. The solvent was removed in *vacuo* and the residue chromatographed by TLC on silica gel. Elution with hexane/CH_2Cl_2 (4:1, v/v) developed three

bands. The first band gave unconsumed starting material (25 mg) while the second and third band afforded $[Ru_4(CO)_{12}(SnPh_3)(\mu\text{-pyS})]$ (**3**) (19 mg, 10%) as violet crystals and $[Ru_2(CO)_4(SnPh_3)_2(\mu\text{-pyS})_2]$ (**1**) (83 mg, 43%) as yellow crystals after recrystallization from hexane/CH_2Cl_2 at 4^{o}C. Spectral data for **1**: Anal. Calcd for $C_{50}H_{38}N_2O_4Ru_2S_2Sn_2$: C, 48.64; H, 3.10; N, 2.27. Found: C, 49.02; H, 3.17; N, 2.31. MS (FAB): *m/z* 1234 (M^+). IR (νCO, CH_2Cl_2): 2029 s, 2016 s, 1968 s, 1956 s cm^{-1}. ^{1}H NMR ($CDCl_3$): δ 7.38 (m, 14H), 7.18 (m, 18H), 6.85 (t, J = 6.4 Hz, 2H), 6.48 (t, J = 6.4 Hz, 2H), 6.02 (d, J = 6.4 Hz, 2H). FAB MS: *m/z* 1234 (M^+), 1206 $(M–CO)^+$, 1178 $(M–2CO)^+$, 1150 $(M–3CO)^+$, 1122 $(M–4CO)^+$. Spectral data for **3**: Anal. Calcd for $C_{35}H_{19}NO_{12}Ru_4SSn$: C, 35.01; H, 1.60; N, 1.17. Found: C, 35.43, H, 1.66; N, 1.20. IR (νCO, CH_2Cl_2): 2098 m, 2039 s, 2021 m, 1997 w, 1968 w cm^{-1}. ^{1}H NMR ($CDCl_3$): δ 8.58 (d, J = 6.0 Hz, 1H), 8.20 (d, J = 6.0 Hz, 1H), 7.57 (m, 7H), 7.31 (m, 9H), 6.68 (t, J = 6.0 Hz). FAB MS: *m/z* 1200 (M^+), 1172 $(M–CO)^+$, 1144 $(M–2CO)^+$, 1088 $(M–4CO)^+$, 976 $(M–8CO)^+$, 920 $(M–10CO)^+$, 864 $(M–12CO)^+$.

2.2. Reaction of 1 with PPh_3 - A benzene solution (20 mL) of **1** (30 mg, 0.024 mmol) and triphenylphosphine (13 mg, 0.049 mmol) was stirred at room temperature for 48 h during which time the color of the reaction mixture changed from yellow to colorless. The solvent was removed under reduced pressure and the residue separated by TLC on silica gel. Elution with hexane/CH_2Cl_2 (1:1, v/v) developed one major and several minor bands. The major band afforded $[Ru(CO)_2(SnPh_3)(PPh_3)(\kappa^2\text{-pyS})]$ (**2**) (37 mg, 87%) as colorless crystals after recrystallization from hexane/CH_2Cl_2 at 4 ^{o}C while the contents of the minor bands were too small for characterization. Spectral data for **2**: Anal. Calcd for $C_{43}H_{34}NO_2PRuSSn$: C, 58.72; H, 3.90; N, 1.59. Found: C, 59.43; H, 3.99; N, 1.65%. IR (νCO, CH_2Cl_2): 2014 vs, 1957 vs cm^{-1}. ^{1}H NMR ($CDCl_3$): δ 7.50(m, 6H) 7.35 (m, 9H), 7.27 (m, 6H), 7.17 (m, 10H), 6.54 (t, J = 7.6 Hz, 1H), 6.08 (t, J = 7.6 Hz, 1H), 5.73 (d, J = 7.6 Hz, 1H); ^{31}P{^{1}H} NMR ($CDCl_3$): δ 29.8 (s). MS (FAB): *m/z* 879 (M^+).

2.3. Reaction of 1 with $[Os_3(CO)_{10}(NCMe)_2]$ - A benzene solution (30 mL) of $[Os_3(CO)_{10}(NCMe)_2]$ (103 mg, 0.110 mmol) and **1** (68 mg, 0.055 mmol) was heated at 70 ^{o}C for 1.5 h. The solvent was removed in *vacuo* and the residue chromatographed by TLC on silica gel. Elution with hexane/CH_2Cl_2 (7:3, v/v) developed one major and several minor bands. The major band afforded $[RuOs_3(CO)_{12}(SnPh_3)(\mu_3\text{-pyS})]$ (**4**) (64 mg, 40%) as red crystals after recrystallization from hexane/CH_2Cl_2 at 4^{o}C while the contents of the minor bands were too small for characterization. Spectral data for **4**: Anal. Calcd for

$C_{35}H_{19}NO_{12}Os_3RuSSn$: C, 28.63; H, 1.30; N, 0.95. Found: C, 28.86, H, 1.35; N, 0.98%. IR (νCO, CH_2Cl_2): 2105 m, 2040 s, 2023 m, 1998 w, 1977 w, 1963 w cm^{-1}. ^1H NMR ($CDCl_3$): δ 8.76 (d, J = 6.0 Hz, 1H), 8.03 (d, J = 6.0 Hz, 1H), 7.59 (m, 7H), 7.31 (m, 9H), 6.63 (t, J = 6.0 Hz, 1H). FAB MS: *m/z* 1469 $[M]^+$, 1413 $(M–2CO)^+$, 1301 $(M–6CO)^+$, 1189 $(M–10CO)^+$. ESI-MS (in MeOH with added NaOMe [37]): *m/z* 1500 $(M+OMe)^–$, 1472 $(M–CO+OMe)^–$.

2.4. Reaction of $[Os_3(CO)_{10}(NCMe)_2]$ with $pySSnPh_3$ - A benzene solution (30 mL) of $[Os_3(CO)_{10}(NCMe)_2]$ (103 mg, 0.110 mmol) and $pySSnPh_3$ (78 mg, 0.169 mmol) was heated to reflux for 3.5 h during which time the color of the reaction mixture changed from yellow to orange. The solvent was removed under reduced pressure and the residue separated by TLC on silica gel. Elution with hexane/CH_2Cl_2 (7:3, v/v) developed one major and several minor bands. The major band afforded $[Os_3(CO)_9(SnPh_3)(\mu_3\text{-pyS})]$ (**5**) (58 mg, 41%) as orange crystals after recrystallization from hexane/$C_2H_4Cl_2$ at 4 ºC. Spectral data for **5**: Anal. Calcd for $C_{32}H_{19}NO_9Os_3SSn$: C, 29.96; H, 1.49; N, 1.09. Found: C, 30.37; H, 1.56; N, 1.14%. IR (νCO, CH_2Cl_2): 2080 s, 2038 vs, 2021 s, 2000 s, 1975 m cm^{-1}. ^1H NMR ($CDCl_3$): δ 9.05 (d, J = 7.6 Hz, 1H), 7.54 (m, 6H), 7.42 (t, J = 7.6 Hz, 1H), 7.31 (m, 9H), 7.05 (t, J = 7.6 Hz, 1H), 6.85 (d, J = 7.6 Hz, 1H). MS (FAB): *m/z* 1283 (M^+).

2.5. Reaction of $[Os_3(CO)_8\{\mu_3\text{-}PPh_2CH_2P(Ph)C_6H_4\}(\mu\text{-}H)]$ with $pySSnPh_3$ - A toluene solution (20 mL) of $[Os_3(CO)_8\{\mu_3\text{-}PPh_2CH_2P(Ph)C_6H_4\}(\mu\text{-}H)]$ (50 mg, 0.042 mmol) and $pySSnPh_3$ (40 mg, 0.087 mmol) was heated to reflux for 2.5 h during which time the color of the reaction mixture changed from green to yellow. The solvent was removed under reduced pressure and the residue separated by TLC on silica gel. Elution with hexane/CH_2Cl_2 (1:1, v/v) developed five bands. The first band was unreacted starting cluster (5 mg) while the second and third bands afforded $[Os_3(CO)_7(SnPh_3)\{\mu\text{-}Ph_2PCH_2P(Ph)C_6H_4\}(\mu\text{-pyS})[(\mu\text{-H})]$ (**7**) (26 mg, 38%) as yellow crystals and $[Os_3(CO)_8(\mu\text{-pyS})(\mu\text{-H})(\mu\text{-dppm})]$ (**6**) (16 mg, 29%) as yellow crystals after recrystallization from hexane/CH_2Cl_2 at 4 ºC. The other two bands were too small for complete characterization. Spectral data for **6**: Anal. Calcd for $C_{38}H_{27}NO_8Os_3P_2S$: C, 35.37; H, 2.11; N, 1.09. Found: C, 35.64; H, 2.18; N, 1.15%. IR (νCO, CH_2Cl_2): 2049 vs, 2014 s, 1989 vs, 1973 sh, 1946 m, 1922 w cm^{-1}. ^1H NMR ($CDCl_3$): δ 8.45 (d, J = 4.6 Hz, 1H), 7.64 (m, 2H), 7.51 (m, 5H), 7.44 (m, 4H), 7.28 (m, 5H), 7.19 (m, 5H), 6.98 (m, 2H), 5.53 (m, 1H), 4.79 (m, 1H), –15.90 (d, J = 30.8 Hz, 1H); $^{31}P\{^1H\}$ NMR ($CDCl_3$): δ –23.4 (d, J = 41.8 Hz, 1P), –24.5 (d, J = 41.8 Hz, 1P). MS (FAB): *m/z* 1291 (M^+). Spectral data for **7**: Anal. Calcd for $C_{55}H_{41}NO_7Os_3P_2SSn$: C, 41.00; H, 2.56; N, 0.87. Found: C, 41.53; H, 2.62; N, 0.91%. IR

(νCO, CH_2Cl_2): 2069 s, 2022 m, 1994 vs, 1953 m, 1933 m cm^{-1}. ^1H NMR ($CDCl_3$): δ 7.84 (m, 6H), 7.67 (m, 2H), 7.59 (m, 1H), 7.48 (m, 3H), 7.31 (m, 6H), 7.16 (m, 11H), 7.08 (m, 2H), 6.97 (m, 2H), 6.76 (m, 2H), 6.65 (m, 1H), 6.18 (m, 2H), 4.96 (m, 1H) 3.86 (m, 1H), –16.62 (dd, J = 16.4, 2.8 Hz, 1H); $^{31}P\{^1H\}$ NMR ($CDCl_3$): δ –5.5 (d, J = 54.1 Hz, 1P), –28.5 (d, J = 54.1 Hz, 1P). MS (FAB): *m/z* 1611 (M^+).

2.6. X-ray Crystallography

Single crystals of **1**, **2**, **4, 5** and **7** suitable for X-ray diffraction were grown by slow diffusion of hexane into a dichloromethane solution at 4 °C. All geometric and crystallographic data were collected at low temperatures (see Table 1) on a Bruker SMART APEX CCD diffractometer using Mo-Kα radiation (λ = 0.71073 Å). Data reduction and integration were carried out with SAINT and absorption corrections were applied using the program SADABS [38]. Structures were solved by direct methods and developed and refined on F^2 using the SHELXL programmes [39] operating under WinGX [40, 41]**.** Hydrogen atoms were included in calculated positions. Crystallographic details are given in Table 1. The determinations were straightforward, except for that of **4**. For this compound the crystal did not diffract well, so the data set was weaker than optimal (I/σ(I) 3.9). The Sn atoms were equally disordered over two sites and this was included in the refinement. The phenyl rings were therefore also disordered but could not be separated into two components so were included as rigid hexagons with isotropic temperature factors. The final difference map showed several large peaks located adjacent to CO ligands which indicated some disorder with these which could not be included sensibly. Hence the determination was less than ideal but overall features are unambiguous.

2.7. Computational Details

Calculations were performed on all derivatives with the Gaussian 03 (G03) program package [42] employing the DFT method with Becke three parameter hybrid functional [43] and Lee-Yang-Parr's gradient corrected correlation functional [44] (B3LYP). The LanL2DZ basis set [45] and effective core potential were used for the Os atoms and the split-valence 6-31G** basis set [46] was applied for all other atoms. The geometry of the clusters, as well as the electronic structures, were calculated in the gas phase. The natural bonding orbital (NBO) method of Weinhold and coworkers [47] was employed for the electronic structure analysis of all compounds.

3. Results and discussion

*3.1. Reaction of $Ru_3(CO)_{12}$ with pyS-$SnPh_3$: synthesis of $[Ru_2(CO)_4(Ph_3Sn)_2(\mu\text{-}pyS)_2]$ (**1**)* - Treatment of $Ru_3(CO)_{12}$ with $pySSnPh_3$ in refluxing benzene gives as the major reaction product the Ru_2Sn_2 complex, $[Ru_2(CO)_4(Ph_3Sn)_2(\mu\text{-}pyS)_2]$ (**1**), isolated as a yellow air-stable crystalline product in 40 % yield (Scheme 2). A minor product (10%) of the reaction is $[Ru_4(CO)_{12}(SnPh_3)(\mu\text{-}pyS)]$ (**3**) discussed below.

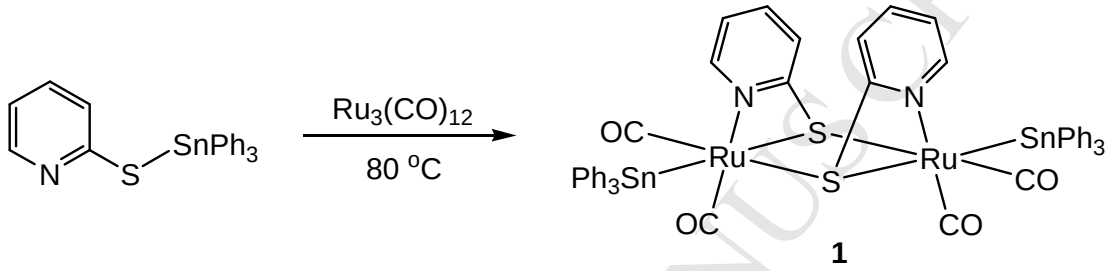

Scheme 2.

The solid-state molecular structure of **1** is shown in Fig. 1 and selected bond distances and angles are listed in the caption. Each ruthenium is also bonded to two carbonyls which are mutually *cis* and a triphenyltin ligand, the latter occupying an equatorial coordination site. Two pyridine-2-thiolate ligands bridge the diruthenium centre to create a non-planar Ru_2S_2 ring with a dihedral angle of 18.9º between the RuS_2 planes and the two $SnPh_3$ ligands, the latter lying approximately *trans* to one another (*anti*). The ruthenium-ruthenium distance of 3.64 Å is clearly non-bonding and each ruthenium atom achieves an 18-electron configuration without such an interaction but considering the pyridine-2-thiolate ligand serves as a five-electron donor. The molecule adopts a chiral structure with C_2 symmetry and the overall structure is very similar to $[M_2(CO)_6(\mu\text{-}pyS)_2]$ (M = Mn, Re) except that one equatorial carbonyl ligand on each metal in these complexes is replaced by the terminal $SnPh_3$ ligands in **1**. The Ru-Sn and Ru-N bond distances in **1** [Ru(1)─Sn(1) 2.6457(2) Å and Ru(2)─Sn(2) 2.6576(2) Å; Ru(1)─N(1) 2.1030(19) Å and Ru(2)─N(2) 2.1259(19) Å] are similar to those found in the literature [20, 21, 30, 48, 49], while the Ru-S bond distances [Ru(1)─S(1) 2.4947(6) Å, Ru(1)─S(2) 2.5241(6) Å, Ru(2)─S(1) 2.5214(6) Å and Ru(2)─S(2) 2.4790(6) Å] are significantly longer than those normally observed in related complexes [48-49]. Spectroscopic

data are fully consistent with the solid-state structure. Notably a single isomer is seen suggesting that the *syn* isomer is sterically disfavored.

*3.2. Cluster **1** as an Ru(CO)$_2$(pyS)(SnPh$_3$) synthon* - In recent work we have shown that the group 7 pyridine thiolate complexes, [M$_2$(CO)$_6$(μ-pyS)$_2$] (M = Mn, Re), act as useful synthons to a range of complexes containing the M(CO)$_3$(pyS) fragment, being especially useful for the rational synthesis of tetranuclear butterfly clusters [50-52]. Given the close structural resemblance of **1** to these complexes we thus considered using the latter as a source of the 16-electron fragment, Ru(CO)$_2$(pyS)(SnPPh$_3$). Indeed this is the case. Treatment of **1** with two equivalents of PPh$_3$ at room temperature resulted in the clean formation of mononuclear [Ru(CO)$_2$(SnPh$_3$)(PPh$_3$)(κ^2-pyS)] (**2**) in essentially quantitative yield (Scheme 3). The ^{31}P{^{1}H} NMR spectrum displays only a singlet at δ 32.8 whereas the FAB mass spectrum shows the parent molecular ion at *m/z* 879. We also determined the single-crystal structure of **2** which is depicted in Fig. 2 with the caption containing selected bond lengths and angles. It has an octahedral arrangement of ligands around the ruthenium atom, with the pyridine thiolate ligand binding in a chelating fashion [N─Ru─S 67.44(6)°]. The triphenyltin and phosphine ligands lie mutually *trans* [P(1)─Ru(1)─Sn(1) 172.96(2)^o], presumably in order to minimise adverse steric interactions and the two carbonyls are in a *cis* orientation. The Ru─N and Ru─Sn bond distances of 2.100(2) Å and 2.6746(5) Å respectively are similar to those found in **1,** while the Ru─S distance of 2.4509(8) Å is slightly shorter than those found in **1**.

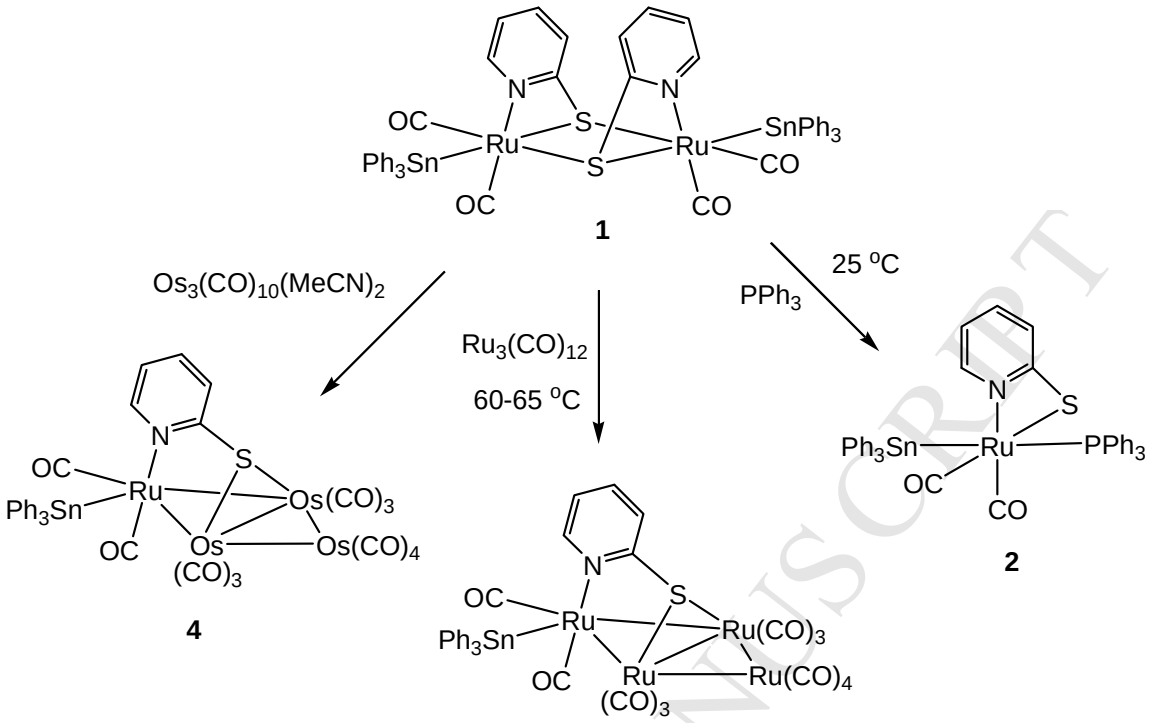

Scheme 3.

As briefly alluded to earlier, a second low yield product of the direct reaction of Ph_3Sn-Spy and $Ru_3(CO)_{12}$ was the cluster $[Ru_4(CO)_{12}(SnPh_3)(\mu\text{-pyS})]$ (**3**). In a separate experiment **1** was shown to smoothly convert into **3** upon addition of further $Ru_3(CO)_{12}$ at between 60-65 ^oC. All attempts to characterize **3** structurally have proved unsuccessful. The FAB mass spectrum shows the expected parent molecular ion at *m/z* 1200 and further ions due to stepwise loss of twelve carbonyl ligands, while the ^1H NMR spectrum displays only aromatic resonances for both phenyl and pyridyl ring protons; two multiplets centered at δ 7.57 (integrated to 6H) and 7.29 (integrated to 9H) are attributed to the phenyl ring protons of $SnPh_3$ moiety, while the doublets at δ 8.58 and 8.20 (J = 5.6 Hz) and the triplets at δ 6.68 and 7.25 (J = 5.6 Hz), each integrating to 1H, are assigned to the ring protons of the pyridine-2-thiolate ligands which supports the structure proposed for **3**.

Heating a benzene solution of **1** and the labile triosmium cluster $[Os_3(CO)_{10}(NCMe)_2]$ at 70 ^oC furnished $[RuOs_3(CO)_{12}(SnPh_3)(\mu_3\text{-pyS})]$ (**4**) in 40% yield (Scheme 3). Spectroscopic data are very similar to that for **3** showing that the two are structurally related. Single crystals of **4** were

grown and the structure of one of the two independent molecules in the asymmetric unit is shown in Figure 3. Ignoring some twisting of the phenyl groups about the tin-carbon bond the other independent molecule is a mirror image, and the following discussion is based on average parameters. The core of the cluster is a 62-electron Os_3Ru butterfly, with the ruthenium atom occupying a wing-tip; the dihedral angle about the hinge being 156º. There are few Os_3Ru butterfly precedents in the Cambridge Crystallographic Database, most of the existing examples having alkyne or other groups bridging the wingtip atoms, and much more acute dihedral angles. Hence **4** with a flattened core structure and a stabilizing ligand attached to the convex face is unique. The pyS ligand is N-bonded to the ruthenium atom and the S atom symmetrically bridges the Os(1)─Os(2) bond which is shorter [2.8011(12)Å] than the two unbridged Os─Os bonds [2.8601(12) Å]. The Ph_3Sn group occupies an equatorial position on the ruthenium atom, and is disordered over two closely adjacent positions arising from slightly different conformations of the phenyl rings, so the Sn─Ru distance of 2.72 Å is not precise but does appear to be significantly longer than the Ru─Sn distances in **1** and **2**. Interestingly the Ru─Os(1) bond *trans* to the Ru─Sn bond is not significantly different to the Ru─Os(2) bond *cis* to it.

3.3. Direct reaction of $[Os_3(CO)_{10}(NCMe)_2]$ with $pySSnPh_3$: synthesis of an Os-Sn bimetallic complex- Reaction of $[Os_3(CO)_{10}(NCMe)_2]$ with $pySSnPh_3$ in refluxing benzene affords the triosmium-tin cluster $[Os_3(CO)_9(SnPh_3)(\mu_3\text{-}pyS)]$ (**5**) in 41% yield (Scheme 4). Compound **5** has been fully characterized by a combination of IR, NMR, mass spectroscopic data and single crystal X-ray diffraction analyses.

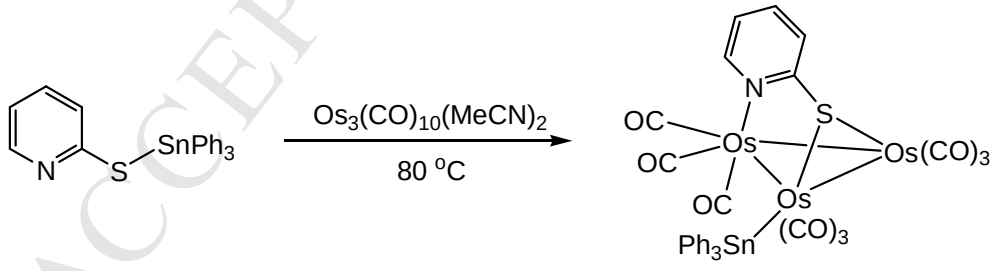

5

Scheme 4.

The solid-state molecular structure of **5** is shown in Fig. 4 and selected bond distances and angles are listed in the caption. The molecule contains a triosmium core with three distinctly different osmium-osmium interactions [Os(1)─Os(2) 2.8090(2) Å, Os(1)─Os(3) 2.8611(2) Å and Os(2)─Os(3) 2.7757(2) Å] ligated by nine carbonyls, a triphenyltin and a pyridine-2-

thiolate ligand. The latter ligand caps a face of the osmium triangle; it bridges Os(1) and Os(2) through the sulfur atom and coordinates to Os(3) through the pyridyl nitrogen atom. The triphenyltin ligand occupies an equatorial position on Os(1) with the Os─Sn bond distance [Os(1)─Sn(1) 2.6856(3) Å] very similar to those found in related triosmium clusters [17-19, 27-29, 30]. The osmium-nitrogen [Os(3)─N(1) 2.183(4) Å] and osmium-sulfur [Os(2)─S(1) 2.401(1) Å & Os(1)─S(1) 2.454(1) Å] distances are within the usual ranges [53-54]. Considering the pyridine-2-thiolate ligand serves as five-electron donor, **5** is an 48-electron cluster with three metal-metal bonds. Spectroscopic data are consistent with the solid-state structure. The aromatic region of the ^{1}H NMR spectrum shows two doublets and two triplets with a relative intensity of 1:1:1:1 due to the ring protons of pyridine-2-thiolate ligand and two multiplets integrated to 15H for the phenyl protons of the triphenyltin ligand. The FAB mass spectrum exhibits the molecular ion at *m/z* 1283 and other ions due to the sequential loss of nine carbonyl ligands.

The difference in isolated products from the reactions of $Ru_3(CO)_{12}$ and $[Os_3(CO)_{10}(MeCN)_2]$ with Ph_3Sn-Spy reflects the well-known enhanced stability of osmium-osmium *vs.* ruthenium-ruthenium bonds. Thus in both reactions the oxidative-addition of the tin-sulfur bond is facile but for osmium the triosmium unit remains intact. A second difference relates to the positioning of the triphenyltin ligand, being at a non-nitrogen bound metal atom in **5**. The mode of formation of **1** and **5** remains unknown. It is tempting to suggest that the first formed species in each case may be $[M_3(CO)_9(\mu_3\text{-pyS-SnPh}_3)]$ in which the capping group acts as a six-electron donor binding through sulfur and nitrogen. Oxidative-addition of the tin-sulfur bond from such a species would directly afford **5**, while for ruthenium a secondary transfer of the tin to the nitrogen bond atom followed by cluster core degradation could afford the labile $Ru(CO)_2(pyS)(SnPh_3)$ fragment which dimerises to form **1**.

3.4. Addition of pySSnPh$_3$ to unsaturated [Os$_3$(CO)$_8${μ_3-PPh$_2$CH$_2$P(Ph)C$_6$H$_4$}(μ-H)] - The electronically unsaturated 46-electron triosmium cluster $[Os_3(CO)_8\{\mu_3\text{-}PPh_2CH_2P(Ph)C_6H_4\}(\mu\text{-H})]$ has been shown to display a rich and varied chemistry [55]. In the context of this work two of its reactions are noteworthy. Thus, addition of pyridine-2-thiol proceeds at room temperature to give thiolate-bridged $[Os_3(CO)_8(\mu\text{-dppm})(\mu\text{-H})(\mu\text{-Spy})]$ (**6**) [56], in which the pyS ligand binds only through sulfur, together with a second product, $[HOs_3(CO)_8\{\mu_3\text{-}PPh_2CH_2P(Ph)C_6H_4\}(\kappa^2\text{-pyS})]$ [56], containing an open array of osmium

atoms and a chelate N,S-pyS ligand. It also reacts at room temperature with triphenyltin to afford $[Os_3(CO)_7(SnPh_3)\{\mu_3\text{-}PPh_2CH_2P(Ph)C_6H_4\}(\mu\text{-}H)_2]$ resulting from oxidative-addition of the tin-hydride bond [17]. Reaction of $[Os_3(CO)_8\{\mu_3\text{-}PPh_2CH_2P(Ph)C_6H_4\}(\mu\text{-}H)]$ with $pySSnPh_3$ in refluxing toluene resulted in the formation of two osmium-tin clusters, $[Os_3(CO)_8(\mu\text{-}pyS)(\mu\text{-}H)(\mu\text{-}dppm)]$ (**6**) and $[Os_3(CO)_7(SnPh_3)\{\mu\text{-}Ph_2PCH_2P(Ph)C_6H_4\}(\mu\text{-}pyS)(\mu\text{-}H)]$ (**7**) in 29 and 38% yield, respectively (Scheme 5). Cluster **6** has previously been reported and was identified by comparison of its spectroscopic data with the literature values [56].

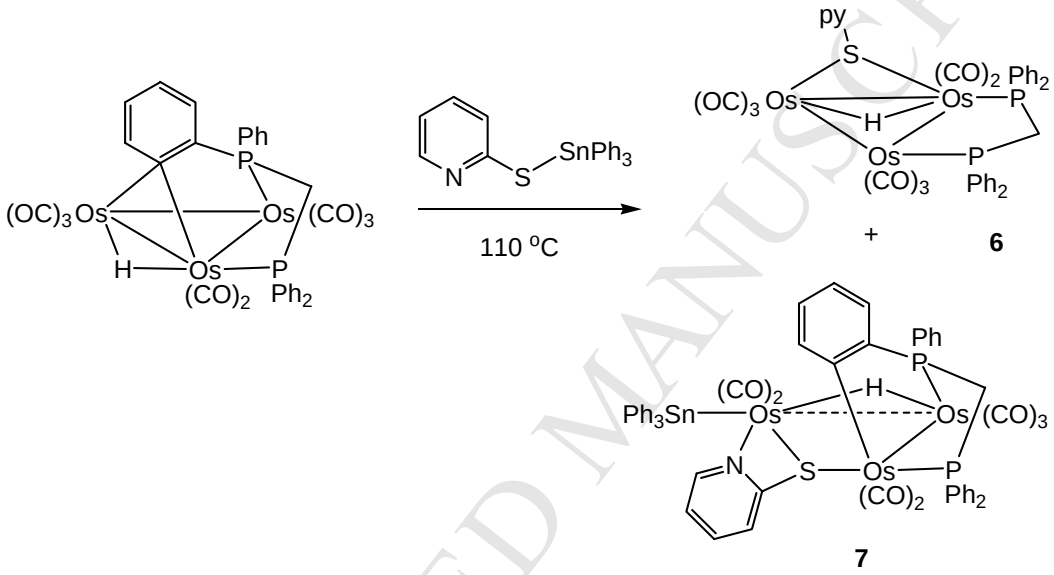

Scheme 5.

The new cluster **7** was characterized by a combination of spectroscopic data and an X-ray crystal structure, the results of which are shown in Fig. 5 with the caption containing selected interatomic distances and angles. It consists of an open triosmium cluster with two quite different osmium-osmium interactions, Os(1)─Os(2) 2.9254(3) Å and Os(2)─Os(3) 3.344(1) Å. The latter is much longer than expected is probably bridged by the hydride (not located) a supposition supported by the ^{1}H NMR spectrum [δ –16.6 (J = 16.4, 2.8 Hz)], the two quite different coupling constants suggesting that the hydride is not located at a similar distance from both phosphorus nuclei. The pyS ligand bridges the open Os(1)─Os(3) edge through the sulfur atom while it coordinates with Os(3) by the ring nitrogen thus forming a four-membered chelate ring. The triphenyltin ligand is equatorially bonded to Os(3). The deprotonated dppm ligand spans the Os(1)─Os(2) edge such that it is equatorially bonded to Os(1) using one phosphorus atom while axially coordinated to Os(2) through the other phosphorus atom to

facilitate the bonding of one of the phenyl rings to Os(1). Spectroscopic data are in accord with the solid-state structure. The $^{31}P\{^{1}H\}$NMR spectrum shows two resonances at δ –5.5 and –28.5 indicating the presence of two non-equivalent phosphorus atoms while the FAB mass spectrum exhibits the molecular ion at *m/z* 1611 and other ions due to the sequential loss of seven carbonyl ligands.

The Os(2)─Os(3) distance of 3.344 Å is long in comparison to conventional osmium-osmium single bond distances and thus in order to get more information about this interaction we have performed DFT calculations on **7** (Supporting Information). A good agreement between the experimental and calculated (3.353 Å) Os(2)─Os(3) distance is found. An electronic structure analysis shows that a direct Os(2)─Os(3) interaction is not present and the two metal centers are rather interacting through the hydride atom. According to natural bonding orbital (NBO) method [47], the hydride atom is binding Os(2) and Os(3) by a delocalizing interaction between its lone pair and two anti-bonding orbitals of Os(2) and Os(3). NBO gives a negative charge of –0.278 and –0.201 to these two atoms respectively, while the charge on the hydride atom is –0.184. A similar type of interaction is also obtained in the canonical molecular orbital description, where the HOMO−1 shows an interaction centered on the hydride atom between a Os(2)−CO anti-bonding orbital and a Os(3)−Sn bonding orbital (Fig. 6).

The mode of formation of **7** is similar to that of **5** formed upon addition of Ph_3Sn-pyS to $[Os_3(CO)_{10}(MeCN)_2]$ but now the cleaved pyridine-thiolate ligand bridges only two metal atoms; probably a result of the sterically demanding nature of the deprotonated dppm ligand. A further difference is the positioning of the triphenyltin ligand which in **7** is bound to the N-bound metal centre.

4. Conclusions

This work has established pyridine-2-thiolate-triphenyltin, Ph_3Sn-Spy, as a source of both triphenyltin and pyridine-2-thiolate ligands *via* the facile sulfur-tin bond cleavage. While in all cases triphenyltin binds in a monodentate fashion, the precise nature of the products obtained varies as a function of the different binding modes of the pyridine-2-thiolate ligand, being found in chelating, bridging and face-capping coordination modes. This suggests that not only will Ph_3Sn-Spy serve as a useful reagent towards the synthesis of tin-containing transition metal clusters but related compounds differing in the nature of the substituent on sulfur are

likely to provide routes into further novel cluster types. An aim of our work in this area is the high yield synthesis of clusters with specific transition metal to tin ratios and geometries for use as precursors towards nano-particulate catalysts and the ability to control these variables in a clear and systematic way is key to the success of this goal.

5. Supporting Information Available

Text, tables and cif files giving details of the X-ray crystallographic structure determinations together with computational details with selected results for **7**. Cif files are also available free of charge via http://www.ccdc.cam.ac.uk/conts/retrieving.html (or from the Cambridge Crystallographic Data Centre) as supplementary publications: CCDC Nos. 795531-795535 for **1, 2, 4, 5, 7**, respectively, 12 Union Road, Cambridge, CB2 1FZ, U.K.: fax: +44-1223-336033; e-mail: deposit@ccdc.cam.ac.uk).

Acknowledgements

This research has been sponsored by the Ministry of Science and Information & Communication Technology, Government of the People's Republic of Bangladesh. We thank Dr Tania Groutso, University of Auckland, for collection of X-ray data.

References

[1] S. Hermans, B.F.G. Johnson, J. Chem. Soc., Chem. Commun. (2000) 1955.
[2] J.M.Thomas, D.W.Lewis, Angew. Chem. Int. Ed. 44 (2005) 6456.
[3] J.M. Thomas, R. Raja, B.F.G. Johnson, S. Hermans, M.D. Jones, T. Khimyak, Ind. Eng. Chem. Res. 42 (2003) 1563.
[4] J.M. Thomas, B.F.G. Johnson, R. Raja, G. Sankar, P.A. Midglcy, Acc. Chem. Res. 36 (2003) 20.
[5] B.F.G. Johnson, Top. Catal. 24 (2003) 147.
[6] R. Srinivasan, B.H. Davis, Platinum Met. Rev. 36 (1992) 151.
[7] R. Bruce, L.C. Garla, J. Catal. 71 (1981) 360.
[8] T. Fujikawa, F.H. Ribciro, G.A. Somorjai, J. Catal. 178 (1998) 58.

[9] R. Bruce, J. Catal. 71 (1981) 348.

[10] M.S. Holt, W.L. Willson, J.H. Nelson, Chem. Rev. 89 (1989) 11.

[11] S. Hermans, R. Raja, J.M. Thomas, B.F.G. Johnson, G. Sankar, D. Gleeson, Angew. Chem. Int. Ed. 40 (2001) 1211.

[12] G.W. Hurber, J.W. Shabaker, J.A. Dumesic, Science 300 (2003) 2075.

[13] B.F.G. Johnson, S.A. Raynor, D.B. Brown, D.S. Shephard, T. Mashmeyer, J.M. Thomas, S. Hermans, R. Raja, G. Sankar, J. Mol. Catal. A: Chem. 182-183 (2002) 89.

[14] A. Hungria, R. Raja, R.D. Adams, B. Captain, J.M. Thomas, P.A. Midgley, V. Golvenko, B.F.G. Johnson, Angew. Chem. Int. Ed. 45 (2006) 969.

[15] K. Burgess, C. Guerin, B.F.G. Johnson, J. Lewis, J. Organomet. Chem. 295 (1985) C3.

[16] W.K. Leong, R.K. Pomeroy, R.J. Batchelor, F.W.B. Einstein, C.F. Compana, Organometallics 15 (1996) 1582.

[17] M.R. Hassan, G. Hogarth, G.M.G. Hossain, S.E. Kabir, A.K. Raha, M.S. Saha, D.A. Tocher, Organometallics 26 (2007) 6473.

[18] R.D. Adams, B. Captain, Z. Lei, Organometallics 25 (2006) 4183.

[19] R.D.Adams, B. Captain, Z. Lei, Organometallics 25 (2006) 2049.

[20] R.D. Adams, D.A. Blom, B. Captain, R. Raja, J.M. Thomas, E. Trufan, Langmuir, 24 (2008) 9223.

[21] R.D. Adams, B. Captain, E. Trufan, J. Organomet. Chem. 693 (2008) 3593.

[22] R.D. Adams, E.M. Boswell, B. Captain, M.A. Patel, Inorg. Chem. 46 (2007) 533.

[23] R.D. Adams, B. Captain, E. Trufan, J. Clust. Sci. 18 (2007) 642.

[24] R.D. Adams, B. Captain, M.A. Patel, M. Johansson, J.L. Smith, Jr. J. Am. Chem. Soc. 127 (2005) 488.

[25] R.J. Hall, P. Serguievski, J.B. Keister, Organometallics 19 (2000) 4499.

[26] F.W.B. Einstein, R.K. Pomeroy, A.C. Willis, J. Organomet. Chem. 3111 (1986) 257.

[27] D.J. Cardin, M.F. Lappert, J. Chem. Soc., Chem. Commun. (1966) 506.

[28] D.J. Cardin, S.A. Keppie, M.F. Lappert, J. Chem. Soc., A (1970) 2594.

[29] J.L. Greàt-Morales, J.M. Fernàndez-G, Organometallics 23 (2004) 3840.

[30] S.E. Kabir, A.K. Raha, M.R. Hassan, B.K. Nicholson, E. Rosenberg, A. Sharmin, L. Salassa, Dalton Trans. (2008) 4212.

[31] S. Ghosh, R. Pervin, A.K. Raha, S.E. Kabir, B.K. Nicholson, Inorg. Chim. Acta 362 (2009) 4226.

[32] G. Hogarth, S.E. Kabir, E. Nordlander, Dalton Transactions, 39 (2010) 6153.

[33] B.F.G. Johnson, J. Lewis, D.A. Pippard, J. Chem. Soc., Dalton Trans. (1981) 407.

[34] J.A. Clucas, D.F. Foster, M.M. Harding, A.K. Smith, J. Chem. Soc., Chem. Commun. (1984) 949.

[35] E.W. Abel, D.B. Brady, J. Chem. Soc. (1965) 1192.

[36] R.C. Pollar "The Chemistry of Organotin Compounds" (1970).

[37] W. Henderson, J.S. McIndoe, B.K. Nicholson, P.J. Dyson, J. Chem. Soc., Dalton Trans. (1998) 519.

[38] R.H. Blessing, Acta Crystallogr., Sect. A, A51 (1995) 33.

[39] G.M. Sheldrick, SHELXL-97, Program for refinement of crystal structures, University of Göttingen, Germany, 1997.

[40] L.J. Farrugia, WinGX, Version 1.70.01, University of Glasgow, UK.

[41] L.J. Farrugia, J. Appl. Crystallogr. 32 (1999) 837.

[42] M.J. Frisch, G.W. Trucks, H.B. Schlegel, G.E. Scuseria, M.A. Robb, J.R. Cheeseman, J.A.Jr. Montgomery, T. Vreven, K.N. Kudin, J.C. Burant, J.M. Millam, S.S. Iyengar, J. Tomasi, V. Barone, B. Mennucci, M. Cossi, G. Scalmani, N. Rega, G.A. Petersson, H. Nakatsuji, M. Hada, M. Ehara, K. Toyota, R. Fukuda, J. Hasegawa, M. Ishida, T. Nakajima, Y. Honda, O. Kitao, H. Nakai, M. Klene, X. Li, J.E. Knox, H.P. Hratchian, J.B. Cross, C. Adamo, J. Jaramillo, R. Gomperts, R.E. Stratmann, O. Yazyev, A.J. Austin, R. Cammi, C. Pomelli, J. Ochterski, P.Y. Ayala, K. Morokuma, G.A. Voth, P. Salvador, J.J. Dannenberg, V.G. Zakrzewski, S. Dapprich, A.D. Daniels, M.C. Strain, O. Farkas, D.K. Malick, A.D. Rabuck, K. Raghavachari, J.B. Forestman, J.V. Ortiz, Q. Cui, A.G. Baboul, S. Clifford, J. Cioslowski, B.B. Stefanov, G. Liu, A. Liashenko, P. Piskorz, I. Komaromi, R.L. Martin, D.J. Fox, T. Keith, M.A. Al-Laham, C.Y. Peng, A. Nanayakkara, M. Challacombe, P.M.W. Gill, B. Johnson, W. Chen, M.W. Wong, C. Gonzales, J.A. Pople, Gaussian 03. (revision D.01). (2004). Wallingford CT, Gaussian Inc.

[43] A.D. Becke, J. Chem. Phys. 98 (1993) 5648.

[44] C. Lee, W. Yang, R.G. Parr, Phys. Rev .B: Condens. Matter 37 (1988) 785.

[45] P.J. Hay, W.R. Wadt, J. Chem. Phys. 82 (1985) 270.

[46] A.D. McLean, G.S. Chandler, J. Chem. Phys. 72 (1980) 5639.

[47] A.E. Reed, L.A. Curtiss, F. Weinhold, Chem. Rev. 88 (1988) 899.

[48] C.J. Cardin, D.J. Cardin, M.A. Convery, Z. Dauter, D. Fenske, M.M. Devereux, M.B. Power, J. Chem. Soc., Dalton Trans. (1996) 1133.

[49] K.M. Hanif, M.S. Islam, S.E. Kabir, K.M.A. Malik, M.A. Miah, N. Wakelin, J. Chem. Crystallogr. 33 (2003) 859.

[50] S. Ghosh, S.E. Kabir, S. Pervin, A.K. Raha, G.M.G. Hossain, D.T. Haworth, S.V. Lindeman, T.A. Siddiquee, D.W. Bennett, L. Salassa, H.W. Roesky, J. Chem. Soc., Dalton Trans. (2009) 3510.

[51] S. Ghosh, K.N. Khanam, M.K. Hossain, G.M.G. Hossain, D.T. Haworth, S.V. Lindeman, G. Hogarth, S.E. Kabir, J. Organomet. Chem. 695 (2010) 1146.

[52] S. Ghosh, K.N. Khanam, G.M.G. Hossain, D.T. Haworth, S.V. Lindeman, G. Hogarth, S.E. Kabir, New J. Chem. 34 (2010) 1875.

[53] S. Ghosh, S.E. Kabir, S. Pervin, A.K. Raha, G.M.G. Hossain, D.T. Haworth, S.V. Lindeman, D.W. Bennett, T.A. Siddiquee, L. Salassa, H.W. Roesky, J. Chem. Soc., Dalton Trans. (2009) 3510.

[54] A.J. Deeming, M.N. Meah, N.P. Randle, K.I. Hardcastle, J. Chem. Soc., Dalton Trans. (1989) 2211.

[55] S.E. Kabir, G. Hogarth, Coord. Chem. Rev. 253 (2009) 1285.

[56] S.E. Kabir, K.M.A. Malik, E. Molla, M.A. Mottalib, J. Organomet. Chem. 616 (2000) 157.

Table 1. Crystallographic Data and Structure Refinement for **1**, **2**, **4, 5** and **7**

Compound	**1**	**2**	**4**	**5**	**7**
Empirical formula	$C_{50}H_{38}N_2O_4Ru_2S_2Sn_2$	$C_{43}H_{34}NO_2PRuSSn$	$C_{35}H_{19}NO_{12}Os_3RuSSn$	$C_{32}H_{19}NO_9Os_3SSn$	$C_{55}H_{41}NO_7Os_3P_2SSn$
Formula weight	1234.46	879.50	1467.93	1282.83	1611.18
Temp (K)	89(2)	150(2)	89(2)	89(2)	150(2)
Wavelength (Å)	0.71073	0.71073	0.71073	0.71073	0.71073
Crystal system	monoclinic	monoclinic	triclinic	triclinic	monoclinic
Space group	$P2_1/c$	$P2_1/c$	*P-1*	*P*-1	$P2_1/c$
a/ Å	10.2388(2)	15.059(2)	12.9069(4)	8.2429(2)	15.886(1)
b/ Å	16.1000(4)	12.584(2)	16.3814(5)	11.6025(3)	25.629(2)
c/ Å	28.0081(6)	20.157(3)	19.3551(7)	18.4101(4)	12.457(11)
α/ °	90	90	103.160(2)	71.908(1)	90
β/ °	95.009(1)	102.463(3)	106.853(2)	82.836(1)	93.902(1)
γ / °	90	90	90.097(2)	82.025(1)	90
V / Å^3	4599.4(2)	3729.7(10)	3803.6(2)	1651.23(7)	5059.9(7)
Z	4	4	4	2	4
D_{calc} (Mg m^{-3})	1.783	1.566	2.563	2.580	2.115
μ (Mo Kα) (mm^{-1})	1.855	1.211	11.137	12.371	8.156
F(000)	2416	1760	2680	1168	3032
Crystal size (mm)	0.30 × 0.28 × 0.16	0.16 × 0.08 × 0.07	0.22 x 0.22 x 0.10	0.28 × 0.20 × 0.14	0.16 × 0.14 × 0.07
θ range (°)	1.46−26.39	2.73−28.30	1.45-27.95	1.86−26.40	2.67−28.30
Index ranges	$-12 \le h \le 12$,	$-19 \le h \le 19$,	$-17 \le h \le 17$	$-10 \le h \le 10$,	$-21 \le h \le 21$,
	$-12 \le k \le 20$,	$-16 \le k \le 16$,	$-21 \le h \le 21$	$-14 \le k \le 14$,	$-34 \le k \le 33$,
	$-35 \le l \le 29$	$-26 \le l \le 26$	$-25 \le h \le 25$	$-23 \le l \le 22$	$-16 \le l \le 16$
Reflections collected	27069	31177	86066	16161	42847

Independent reflections (R_{int})	9393 (0.0186)	8897(0.0350)	17992(0.0956)	6727(0.0213)	12112(0.0441)
Max. and min. transmission	0.7556 and 0.6060	0.9200 and 0.8298	0.4022 and 0.1931	0.198 and 0.127	0.5991 and 0.3553
Data/restraints/parameters	9393/0/559	8897/0/451	17992/48/739	6727/0/424	12112/0/631
Goodness-of-fit on F^2	1.094	1.024	1.094	1.022	1.014
Final R indices [$I > 2\sigma(I)$]	R_1 = 0.0210,	R_1 = 0.0332,	R_1 = 0.0653	R_1 = 0.0211,	R_1 = 0.0310,
	wR_2 = 0.451	wR_2 = 0.0764	wR_2 = 0.1542	wR_2 = 0.0466	wR_2 = 0.0663
R indices (all data)	R_1 = 0.0256,	R_1 = 0.0441,	R_1 = 0.1588	R_1 = 0.0233,	R_1 = 0.0399,
	wR_2 = 0.469	wR_2 = 0.0802	wR_2 = 0.2213	wR_2 = 0.0476	wR_2 = 0.0691
Largest difference in peak and hole (e Å^{-3})	0.61 and −0.61	1.32 and −0.44	5.91 and -2.70	1.13 and −1.23	1.54 and −0.94

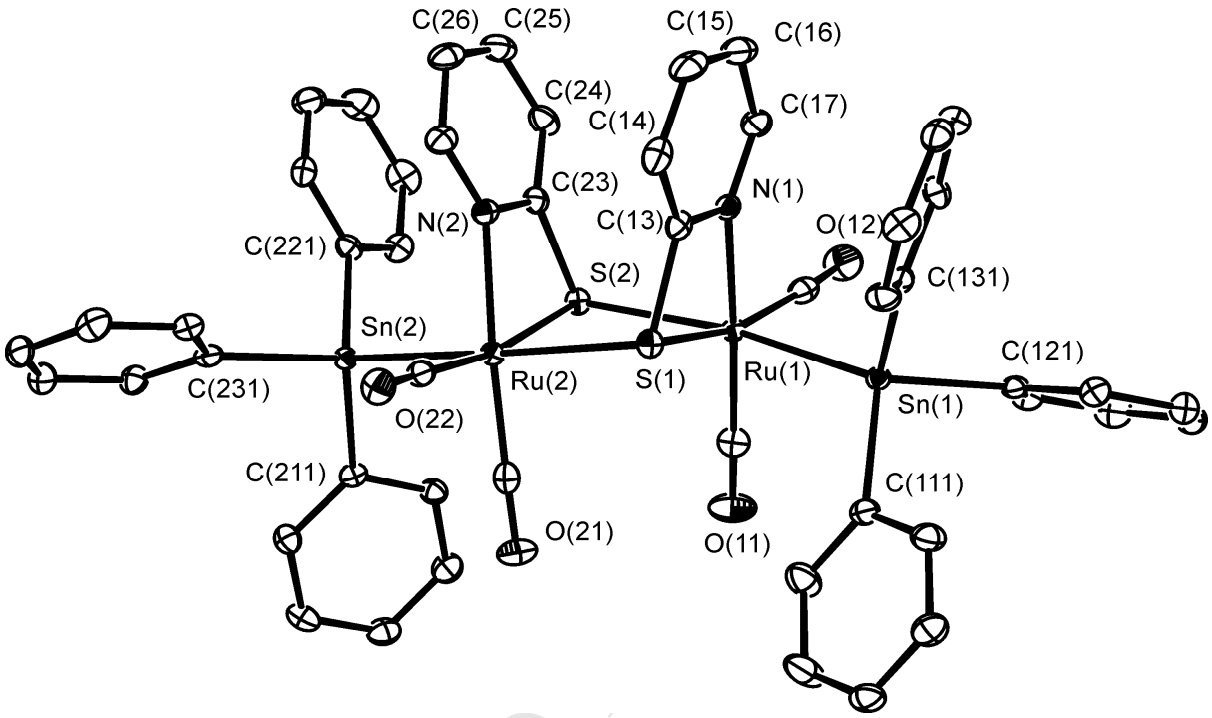

Fig. 1. Molecular structure of $[Ru_2(CO)_4(Ph_3Sn)_2(\mu\text{-}pyS)_2]$ (**1**) (thermal ellipsoids at 50% probability). Selected interatomic distances (Å) and angles (º): Ru(1)─Sn(1) 2.6457(2), Ru(2)─Sn(2) 2.6576(2), Ru(1)─S(1) 2.4947(6), Ru(1)─S(2) 2.5241(6), Ru(2)─S(1) 2.5214(6), Ru(2)─S(2) 2.4790(6), Ru(1)─N(1) 2.103(2), Ru(2)─N(2) 2.126(2), N(1)─Ru(1)─S(1) 67.06(5), N(1)─Ru(1)─S(2) 90.02(5), S(1)─Ru(1)─S(2) 84.96(2), N(1)─Ru(1)─Sn(1) 88.73(5), Ru(1)─S(1)─Ru(2) 93.02(2).

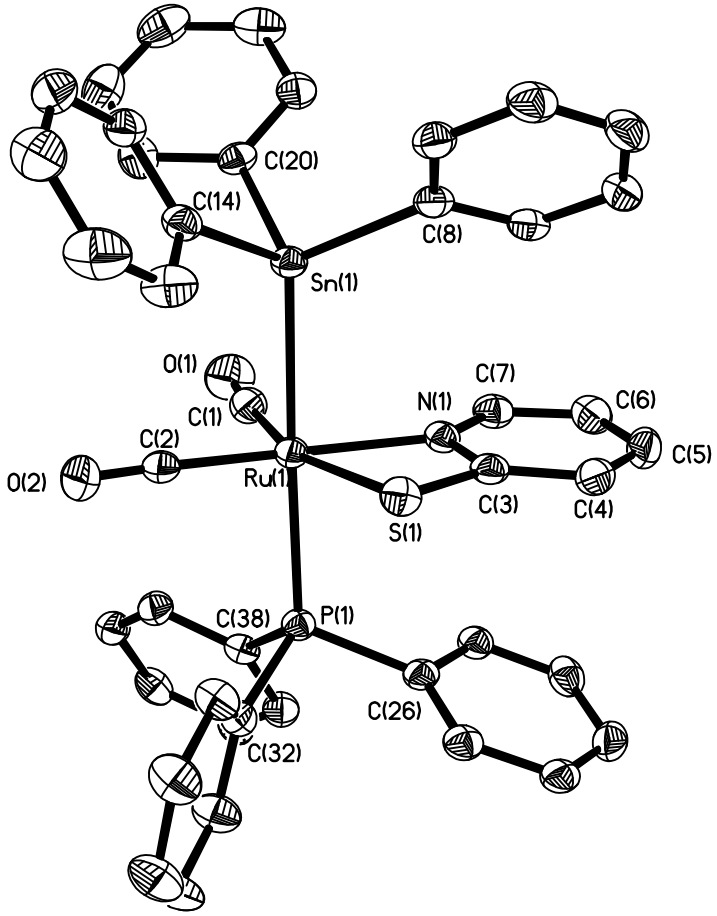

Fig. 2. Molecular structure of $[Ru(CO)_2(SnPh_3)(PPh_3)(\kappa^2\text{-pyS})$ (**2**) (thermal ellipsoids at 50% probability). Hydrogen atoms have been omitted for clarity. Selected interatomic distances (Å) and angles (º): Ru(1)─Sn(1) 2.6746(5), Ru(1)─S(1) 2.4509(8), Ru(1)─N(1) 2.100(2), Ru(1)─P(1) 2.4177(7), N(1)─Ru(1)─S(1) 67.44(6), N(1)─Ru(1)─P(1) 90.73(6), P(1)─Ru(1)─S(1) 86.60(2), P(1)─Ru(1)─Sn(1) 172.96(2), N(1)─Ru(1)─Sn(1) 89.12(5), S(1)─Ru(1)─Sn(1) 86.84(2), C(1)─Ru(1)─N(1) 96.1(1), C(2)─Ru(1)─C(1) 94.2(1).

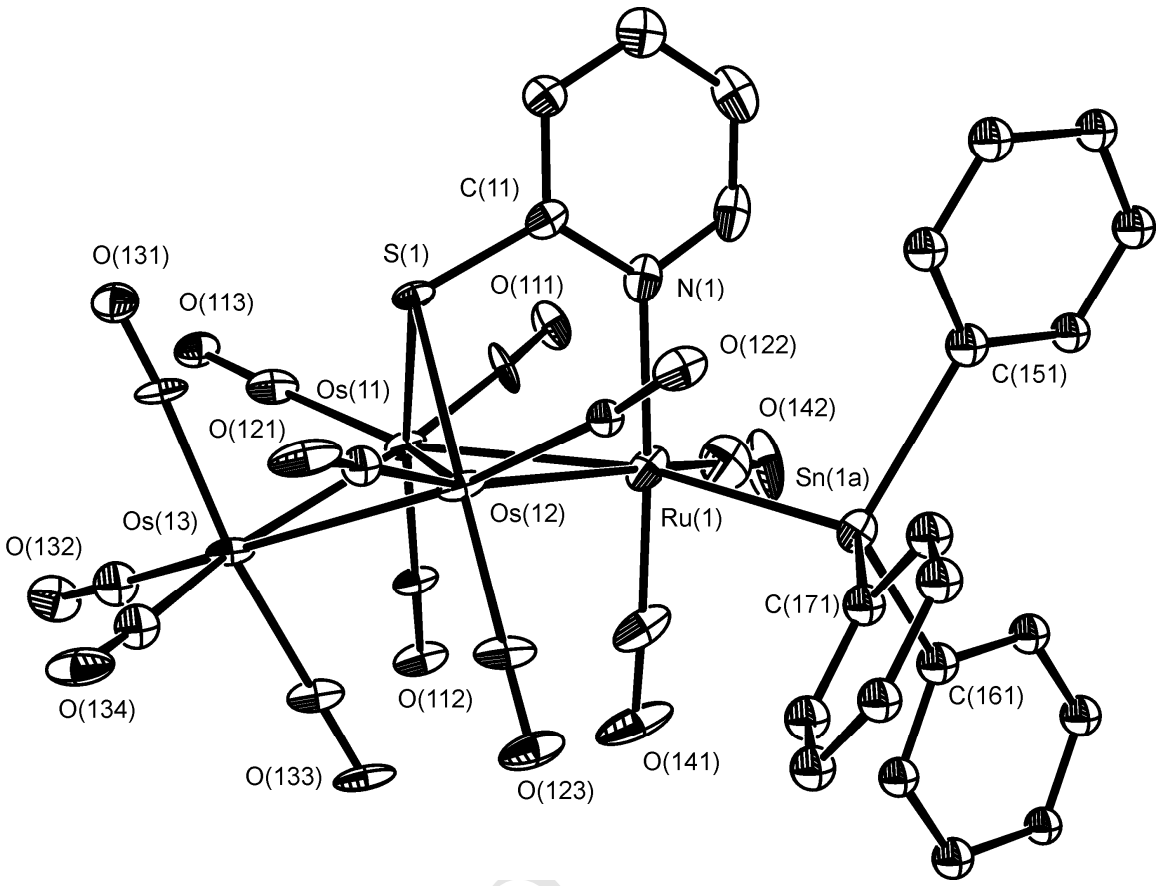

Fig. 3. Molecular structure of one of the independent molecules of $[Os_3Ru(CO)_{12}(SnPh_3)(\mu_3\text{-}pyS)]$ (**4**) (thermal ellipsoids at 35% probability). Only one of the two disordered tin atoms is shown. Selected interatomic distances (Å) and angles (º) (for independent molecules 1 and 2 in each case): Os(1)─Os(2) 2.7995(9) 2.8027(9), Os(2)─Os(3) 2.867(1) 2.870(1), Os(1)─Os(3) 2.855(1) 2.870(1), Os(1)─Ru(1) 2.921(2) 2.868(2), Os(2)─Ru(1) 2.863(2) 2.899(2) Ru(1)─Sn(1) 2.72 2.72, Os(1)─S 2.411(4) 2.400(4), Os(2)─S 2.403(4) 2.401(4), Ru(1)─N 2.19(2) 2.20(2). Dihedral angle between Os_3 and Os_2Ru planes 156.3, 156.1º.

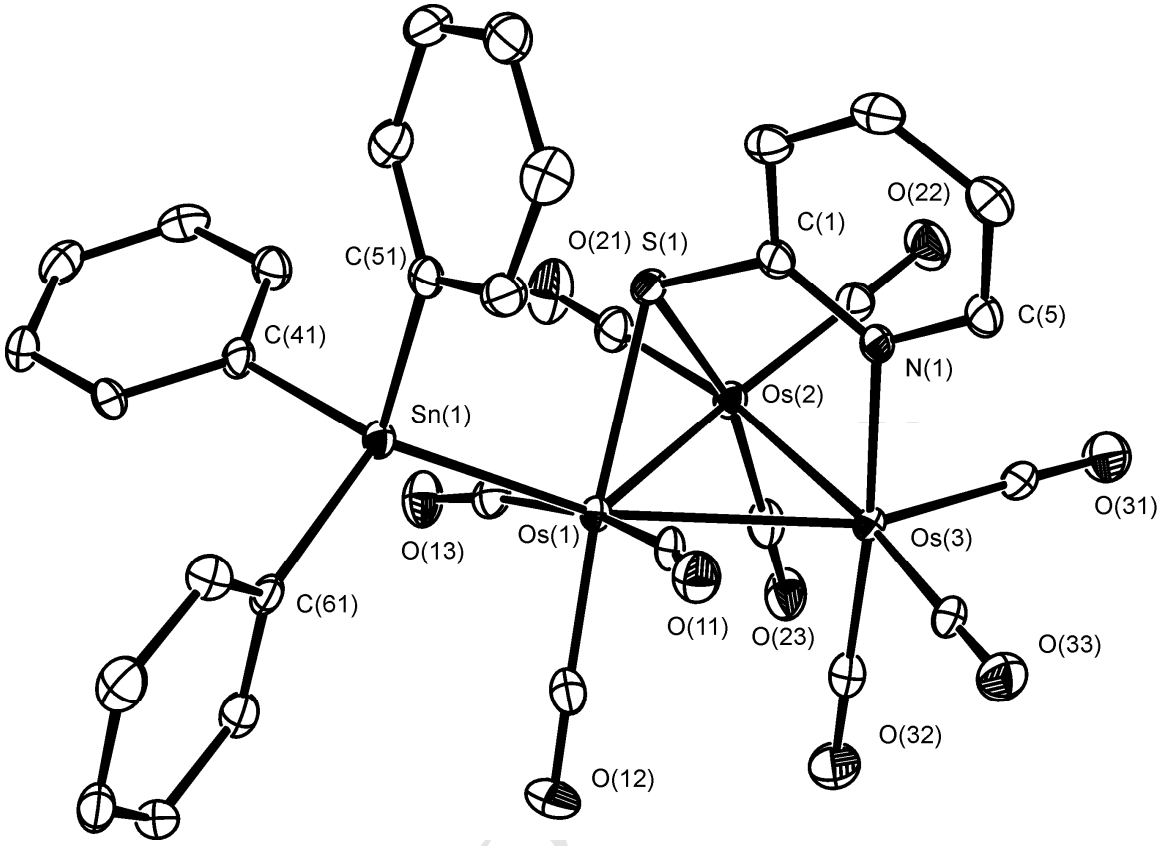

Fig. 4. Molecular structure of $[Os_3(CO)_9(SnPh_3)(\mu_3\text{-pyS})]$ (**5**) (thermal ellipsoids at 50% probability). Selected interatomic distances (Å) and angles (º): Os(1)─Sn(1) 2.6856(3), Os(1)─Os(2) 2.8090(2), Os(1)─Os(3) 2.8611(2), Os(2)─Os(3) 2.7757(2), Os(1)─S(1) 2.4544(11), Os(2)─S(1) 2.4009(11), Os(3)─N(1) 2.183(4), Os(1)─Os(2)─Os(3) 61.633(6), Os(1)─Os(3)─Os(2) 59.756(6), Os(2)─Os(1)─Os(3) 58.611(6), S(1)─Os(1)─Sn(1) 86.54(3), S(1)─Os(1)─Os(2) 53.77(3), Sn(1)─Os(1)─Os(3) 146.37(1), Sn(1)─Os(1)─Os(2) 132.21(1), N(1)─Os(3)─Os(1) 87.52(9), Os(2)─S(1)─Os(1) 70.68(3).

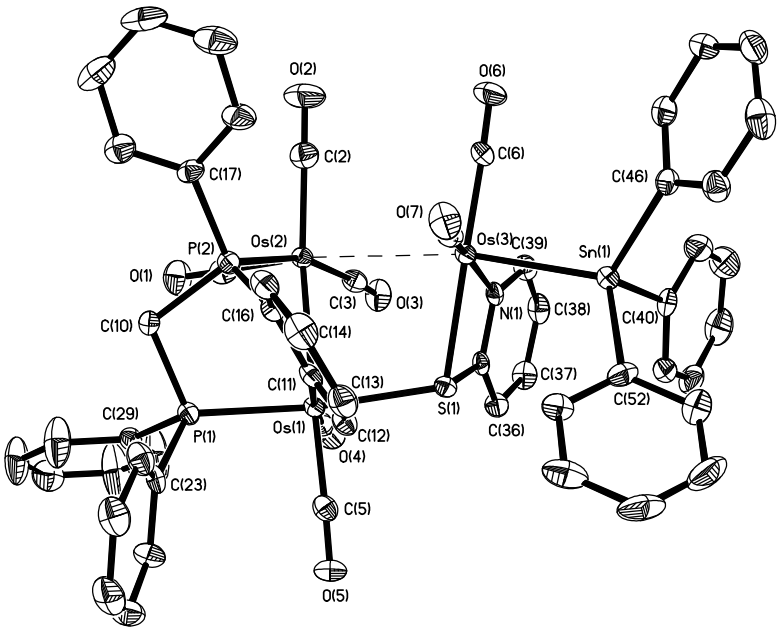

Fig. 5. Molecular structure of $[Os_3(CO)_7(SnPh_3)\{\mu\text{-}Ph_2PCH_2P(Ph)C_6H_4\}(\mu\text{-}pyS)(\mu\text{-}H)]$ (**7**) (thermal ellipsoids at 50% probability). Hydrogen atoms have been omitted for clarity. Selected interatomic distances (Å) and angles (º): Os(3)─Sn(1) 2.6731(4), Os(1)─Os(2) 2.9254(3), Os(2)─Os(3) 3.344(1), Os(1)─S(1) 2.4643(12), Os(3)─S(1) 2.474(1), Os(3)─N(1) 2.113(4), Os(1)─C(11) 2.167(4), Os(1)─P(1) 2.3282(12), Os(2)─P(2) 2.3533(11), Os(1)─Os(2)─Os(3) 55.2º, Os(1)─S(1)─Os(3) 108.11(4), C(11)─Os(1)─S(1) 85.2(1), C(11)─Os(1)─Os(2) 89.6(1), P(1)─Os(1)─S(1) 162.25(4), P(1)─Os(1)─Os(2) 90.44(3), N(1)─Os(3)─S(1) 66.8(1), S(1)─Os(3)─Sn(1) 90.56(3), N(1)─Os(3)─Sn(1) 86.8(1).

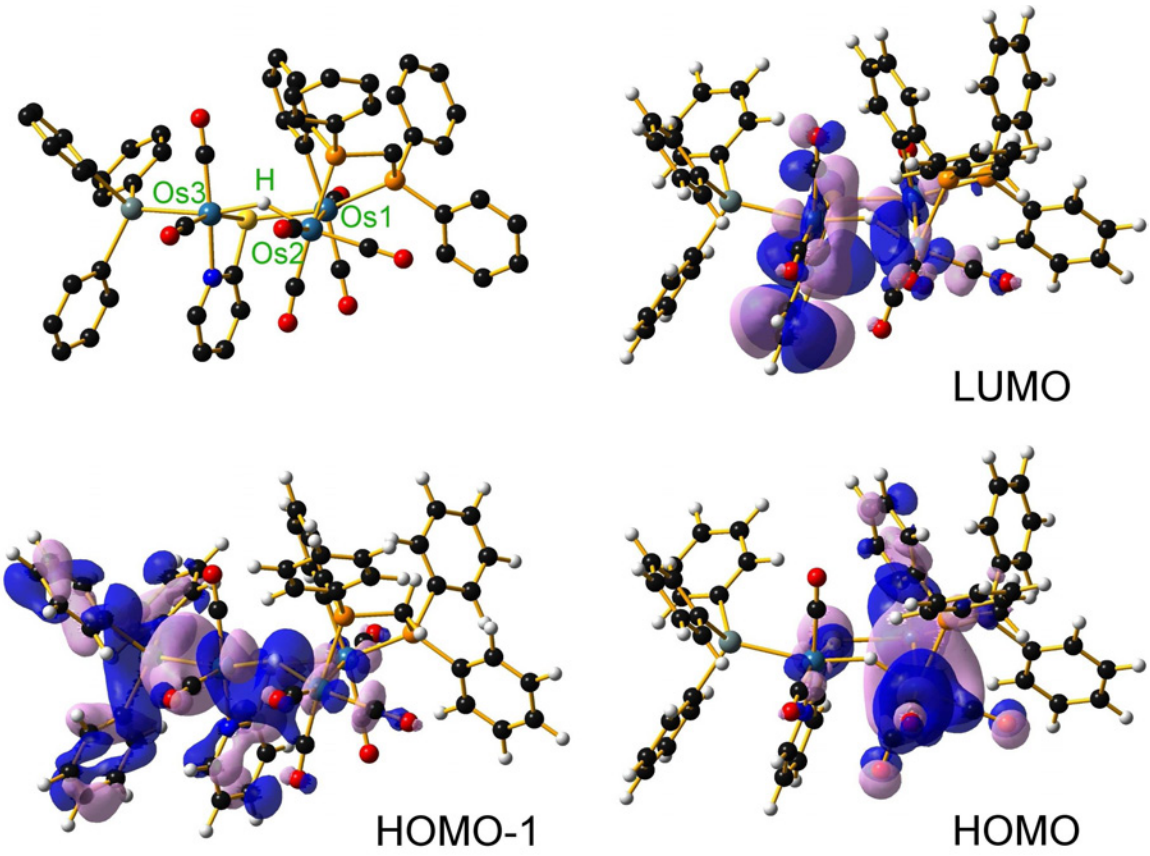

Fig. 6. Schematic structure (drawn without H atoms, except hydride) and selected molecular orbitals of $[Os_3(CO)_7(SnPh_3)\{\mu\text{-}Ph_2PCH_2P(Ph)C_6H_4\}(\mu\text{-}pyS)(\mu\text{-}H)]$ (**7**).

Graphical Abstract

Synthesis of new heterometallic complexes by tin-sulfur bond cleavage of $pySSnPh_3$ (pySH = pyridine-2-thiol) at triruthenium and triosmium centres

Arun K. Raha, Shishir Ghosh, Iqbal Hossain, Brian K. Nicholson, Graeme Hogarth, Luca Salassa and Shariff E. Kabir

The reactivity of $pySSnPh_3$ with triruthenium and triosmium carbonyl clusters has been investigated. A number of novel clusters enriched with tin and sulfur donor ligands have been obtained.

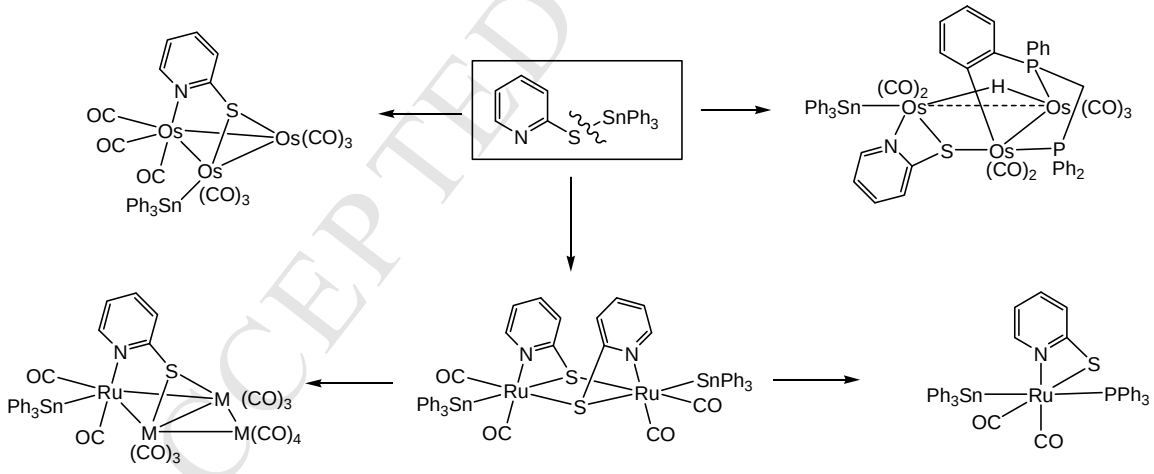

Tin-sulfur bond cleavage of py$SSnPh_3$ at triruthenium and triosmium centres;

Synthesis of heterometallic clusters;

Synthesis of butterfly clusters